Article

SCIENCE PROGRESS

Science Progress
2021, Vol. 104(3) 1–15

DOI: 10.1177/00368504211031693
journals.sagepub.com/home/sci
SAGE

Mechanics of non-Newtonian blood flow in an artery having multiple stenosis and electroosmotic effects

Salman Akhtar[1], Luthais B McCash[2], Sohail Nadeem[1], Salman Saleem[3] and Alibek Issakhov[4]

[1]Department of Mathematics, Quaid-i-Azam University, Islamabad, Pakistan
[2]Department of Actuarial Sciences, University of Leicester, Leicester, UK
[3]Department of Mathematics, King Khalid University, Abha, Saudi Arabia
[4]Department of Mechanics, Al-Farabi Kazakh National University, Almaty, Kazakhstan

Abstract

The electro-osmotically modulated hemodynamic across an artery with multiple stenosis is mathematically evaluated. The non-Newtonian behaviour of blood flow is tackled by utilizing Casson fluid model for this flow problem. The blood flow is confined in such arteries due to the presence of stenosis and this theoretical analysis provides the electro-osmotic effects for blood flow through such arteries. The mathematical equations that govern this flow problem are converted into their dimensionless form by using appropriate transformations and then exact mathematical computations are performed by utilizing Mathematica software. The range of the considered parameters is given as $0.03 < \delta_l < 0.12, 2 < m < 3.5, 0.03 < Q < 2, \quad 0 < U_{HS} < 3, 2 < B_r < 2.9,$ $0.01 < S < 0.025$. The graphical results involve combine study of symmetric and non-symmetric structure for multiple stenosis. Joule heating effects are also incorporated in energy equation together with viscous effects. Streamlines are plotted for electro-kinetic parameter m and flow rate Q. The trapping declines in size with incrementing m, for symmetric shape of stenosis. But the size of trapping increases for the non-symmetric case.

Keywords

Electro-osmosis, multiple stenosis, Casson fluid, Joule heating

Corresponding author:
Sohail Nadeem, Department of Mathematics, Quaid-i-Azam University, Islamabad 45320, Pakistan.
Email: sohail@qau.edu.pk

Introduction

The electro-osmotic phenomenon emerges when a channel under consideration is filled with an electrolyte solution and then by application of a high voltage, a charge is produced at inner surface of this tube when this electrolyte comes in contact with inner walls. Finally, the flow is developed due to this electric field.[1] Electro-osmosis has immense uses in medical field and helps in treatment of diseases like cellular anomalies, sickle cells, and delivery of drugs by using diagnostic kits.[2] The capillary electro-kinetic detailed study and various micro-chip methods are addressed.[3] Wu and Papadopoulos[4] had presented a mathematical model that compares the cylindrical and annulur electro-kinetic flows. The electro-kinetically produced flow between two parallel plates was mathematically studied by Yang et al.[5] Zhao et al.[6] had mathematically examined the two dimensional flow of a power law fluid by application of electroosmosis. The electro-kinetic flow of non-Newtonian fluids in small length tubes was first time interpreted by Tang et al.[7] Liu et al.[8] had interpreted the micro-slit channel flow using Jeffery fluid model by utilizing electro-kinetic mechanism. The Bingham plastic fluid's electro-osmotic flow across a micro length channel was mathematically examined by Nadeem et al.[9] Some of the recent research articles that interpret the electro-osmotic flow phenomenon are referred by Narla and Tripathi,[10] Tripathi et al.,[11] Akram et al.,[12] and Saleem et al.[13]

The blood arteries with stenosis result in restriction of hemodynamics across these diseased arteries. In some certain conditions, such arteries may also have more than one stenosis. The study of flow across such multiple stenosed arteries is also a topic of recent interest for researchers. The flow across such stenosed arteries was firstly reported by Ponalagusamy[14] in his doctoral dissertation. This arterial study of mild stenosis is also covered for stenosis with various shapes.[15] Varshney et al.[16] had presented the mathematical study of a non-Newtonian fluid flow across a channel with multiple stenosis. Sreenadh et al.[17] had studied the flow of blood across a multiple stenosed tube, treating blood as a Casson fluid. Nadeem and Ijaz[18] had mathematically examined the blood flow across a multiple stenosed tube with variable fluid properties. The blood flow across such diseased multiple stenosed arteries, considering distinct models of non-Newtonian fluids is given.[19–27]

The heat transfer study of blood flow across an artery with multiple stenosis was interpreted by Tashtoush and Magableh.[28] The analysis of heat phenomenon for a mild stenotic tube, considering two phase blood flow model was conveyed by Ponalagusamy and Selvi.[29] The heat transfer analysis of Williamson blood flow model for a stenotic tube was mathematically interpreted by Akbar et al.[30] The heat transfer details combined with dissipation effects and Joule heating for an electro-kinetically developed flow was studied by Sadeghi and Saidi.[31] Moreover, some further recent researches that evaluate blood flow as well as heat transfer are referred by Yan et al.,[23] Li et al.,[32] Ho et al.,[33,34] and Chien et al.,[35]

The review of literature has shown that the electro-osmotic flow of blood across a multiple stenosed artery is not mathematically considered yet. We have analyzed the electro-kinetic flow of blood across an artery with multiple stenosis. The non-

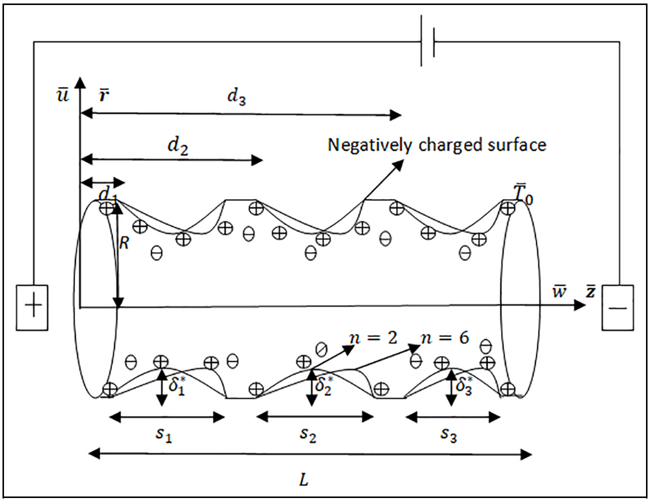

Figure 1. Geometry of the problem.

Newtonian behavior of blood is incorporated by using Casson fluid model for this problem. In order to describe a thorough heat transfer mechanism, Joule heating effect is also incorporated together with viscous dissipation. Exact mathematical solutions are prevailed for governing flow equations. Further, these results are studied in detail with graphs.

Mathematical model

The electro-osmotically driven hemodynamic across an artery with multiple stenosis is studied. The non-Newtonian behaviour of blood is considered by utilizing Casson model for this flow problem.

The multiple stenosis wall geometry $\bar{\eta}(z)$, with its dimensional mathematical expression (Figure 1).[36]

$$\bar{\eta}(z) = \begin{cases} R\left[1 - \mathrm{K}\left\{s_l^{n-1}(\bar{z} - d_l) - (\bar{z} - d_l)^n\right\}\right], d_l \le \bar{z} \le d_l + s_l \\ R \qquad\qquad\qquad\qquad\qquad\qquad\qquad\quad otherwise, \end{cases}. \tag{1}$$

The expression for value of K is

$$\mathrm{K} = \frac{\delta_l^*}{R s_l^n} \frac{n^{n/n-1}}{n-1}, \tag{2}$$

The governing mathematical equations that manipulate the incompressible flow of Casson fluid are

$$\frac{\partial \bar{u}}{\partial \bar{r}} + \frac{\bar{u}}{\bar{r}} + \frac{\partial \bar{w}}{\partial \bar{z}} = 0, \tag{3}$$

$$\rho\left(\bar{u}\frac{\partial \bar{u}}{\partial \bar{r}} + \bar{w}\frac{\partial \bar{u}}{\partial \bar{z}}\right) = -\frac{\partial \bar{p}}{\partial \bar{r}} + \frac{1}{\bar{r}}\frac{\partial}{\partial \bar{r}}(\bar{r}\bar{S}_{\bar{r}\bar{r}}) + \frac{\partial}{\partial \bar{z}}(\bar{S}_{\bar{r}\bar{z}}), \tag{4}$$

$$\rho\left(\bar{u}\frac{\partial \bar{w}}{\partial \bar{r}} + \bar{w}\frac{\partial \bar{w}}{\partial \bar{z}}\right) = -\frac{\partial \bar{p}}{\partial \bar{z}} + \frac{1}{\bar{r}}\frac{\partial}{\partial \bar{r}}(\bar{r}\bar{S}_{\bar{r}\bar{z}}) + \frac{\partial}{\partial \bar{z}}(\bar{S}_{\bar{z}\bar{z}}) + \rho_e E_z, \tag{5}$$

$$\rho C_p\left(\bar{u}\frac{\partial \bar{T}}{\partial \bar{r}} + \bar{w}\frac{\partial \bar{T}}{\partial \bar{z}}\right) = \bar{S}_{\bar{r}\bar{r}}\frac{\partial \bar{u}}{\partial \bar{r}} + \bar{S}_{\bar{r}\bar{z}}\frac{\partial \bar{w}}{\partial \bar{r}} + \bar{S}_{\bar{z}\bar{r}}\frac{\partial \bar{u}}{\partial \bar{z}} + \bar{S}_{\bar{z}\bar{z}}\frac{\partial \bar{w}}{\partial \bar{z}} + k\left(\frac{\partial^2 \bar{T}}{\partial \bar{r}^2} + \frac{1}{\bar{r}}\frac{\partial \bar{T}}{\partial \bar{r}} + \frac{\partial^2 \bar{T}}{\partial \bar{z}^2}\right) + s^*, \tag{6}$$

The Casson fluid's extra stress tensor.[37] The Casson fluid model is chosen to consider the non-Newtonian nature of blood.

$$\bar{S}_{ij} = \left(\mu_B + \frac{p_y}{\sqrt{2\pi_c}}\right)\bar{e}_{ij}, \tag{7}$$

Where

$$\bar{e}_{ij} = \frac{\partial \bar{v}_i}{\partial \bar{x}_j} + \frac{\partial \bar{v}_j}{\partial \bar{x}_i}, \tag{8}$$

The value of s^* given in equation (6) is $s^* = i_e^2\sigma,$ where $i_e = \frac{E_z}{\sigma}$.[38] An electrolyte mixture ($Na^+ Cl^-$) is uniformly considered and it's electrical potential dispersion is mathematically expressed by Poisson-Boltzmann equation as

$$\nabla^2\bar{\Phi} = -\frac{\rho_e}{E}, \tag{9}$$

The value of $\rho_e = ez^*(n^+ - n^-),$ the density of ionic energy, when "no EDL overlap" is considered, is given

$$n^{\pm} = n_0 Exp \pm \left(ez^*\bar{\Phi}/K_B T^*\right), \tag{10}$$

Now substituting the value of ρ_e and $n^{\pm}$ in equation (9), we get

$$\frac{1}{\bar{r}}\frac{\partial}{\partial \bar{r}}\left(\bar{r}\frac{\partial \bar{\Phi}}{\partial \bar{r}}\right) = \frac{2n_0 ez^* Sinh\left(ez^*\bar{\Phi}/K_B T^*\right)}{E}, \tag{11}$$

The Debye-Huckel approximation is utilized and we get $Sinh(ez^*\bar{\Phi}/K_B T^*) \approx ez^*\bar{\Phi}/K_B T^*$. Also the non-dimensional variables $\Phi = \bar{\Phi}/\zeta, r = \bar{r}/R$ are used in equation (11) and we get

$$\frac{1}{r}\frac{\partial}{\partial r}\left(r\frac{\partial \Phi}{\partial r}\right) = m^2\Phi, \tag{12}$$

The Exact solution of equation (12) is obtained with these conditions $\frac{\partial \Phi}{\partial r} = 0, atr = 0,$ and $\Phi = 1atr = \eta(z)$.

$$\Phi = {I_0(mr)}/{I_0(m\eta)}, \tag{13}$$

The variables used in their dimensionless form are

$$r = \frac{\bar{r}}{R}, z = \frac{\bar{z}}{s_l}, w = \frac{\bar{w}}{u_0}, u = \frac{L\bar{u}}{u_0\delta_l^*}, p = \frac{R^2\bar{p}}{u_0 s_l \mu_f}, \theta = \frac{\bar{T} - \bar{T}_0}{\bar{T}_0},$$

$$\eta(z) = \frac{\bar{\eta}(z)}{R}, h_l = \frac{d_l}{s_l}, \delta_l = \frac{\delta_l^*}{R}, S = \frac{E_z^2 R^2}{\sigma \bar{T}_0 k}, B_r = \frac{\mu_f u_0^2}{k_f \bar{T}_0},$$

$$m = Rez^*\sqrt{{2n_0}/{EK_B T^*}} = \frac{R}{\lambda_d}, U_{HS} = \frac{E_z E\zeta}{\mu u_0}, \beta = \frac{\mu_B\sqrt{2\pi_c}}{p_y}, S_{ij} = \frac{R\bar{S}_{ij}}{u_0\mu_f}, \tag{14}$$

The following assumptions are used in this study, in order to consider mild case of multiple stenosis

$$\delta_l = \frac{\delta_l^*}{R} \ll 1, \frac{Rn^{1/n} - 1}{s_l} \sim^\circ 1 \tag{15}$$

The dimensionless variables provided in equation (14) and assumptions in equation (15) are used to get these dimensionless equations

$$\frac{\partial p}{\partial r} = 0, \tag{16}$$

$$\frac{\partial p}{\partial z} = \left(1 + \frac{1}{\beta}\right)\left(\frac{\partial^2 w}{\partial r^2} + \frac{1}{r}\frac{\partial w}{\partial r}\right) + m^2 U_{HS}\frac{I_0(mr)}{I_0(m\eta)}, \tag{17}$$

$$\frac{\partial^2 \theta}{\partial r^2} + \frac{1}{r}\frac{\partial \theta}{\partial r} + \left(1 + \frac{1}{\beta}\right)B_r\left(\frac{\partial w}{\partial r}\right)^2 + S = 0, \tag{18}$$

The relevant dimensionless form of boundary conditions is

$$\frac{\partial w}{\partial r} = 0atr = 0andw = 0atr = \eta, \tag{19}$$

$$\frac{\partial \theta}{\partial r} = 0atr = 0and\theta = 0atr = \eta, \tag{20}$$

The dimensionless mathematical form of multiple stenosis wall is

$$\eta(z) = \begin{cases} 1 - \delta_l \frac{n^{n/n-1}}{n-1}[(z-h_l)-(z-h_l)^n], h_l \le z \le h_l + 1 \\ 1 otherwise \end{cases}, \tag{21}$$

Exact solution

The mathematical solution of axial velocity is

$$w(r,z) = \frac{\beta\left[4U_{HS} + \frac{dp}{dz}(r^2 - \eta^2) - \frac{4U_{HS}I_0(mr)}{I_0(m\eta)}\right]}{4(1+\beta)}, \tag{22}$$

The volume rate of flow is evaluated by considering

$$Q = 2\pi \int_0^\eta rwdr, \tag{23}$$

Thus, the mathematical result for pressure gradient is

$$\frac{dp}{dz} = \frac{8}{\eta^4}\left[-\frac{Q(1+\beta)}{\pi\beta} + U_{HS}\eta^2 - \frac{2U_{HS}\eta I_1(m\eta)}{mI_0(m\eta)}\right], \tag{24}$$

The shear stress at multiple stenosed wall is provided

$$\tau_w = -\frac{\partial w}{\partial r}\bigg|_{r=\eta} = -\frac{\beta\left[2\frac{dp}{dz}\eta - \frac{4mU_{HS}I_1(m\eta)}{I_0(m\eta)}\right]}{4(1+\beta)}, \tag{25}$$

The exact temperature profile solution is

$$\theta(r,z) = \frac{1}{64m^2(1+\beta)(I_0(m\eta))^2} \tag{26}$$

Results and discussion

The mathematical solutions acquired in above portion are explained in detail with graphical results. In Figure 2(a)–(d), the velocity graphs are represented for enlarging values of distinct physical parameters. It is observed in Figure 2(a) that there is enhance in velocity at the centre, as the value of δ_l increases but it declines toward walls with multiple stenosis. The velocity gains magnitude due to narrowing of channel with incrementing δ_l but at the same time velocity reduces toward walls with multiple stenosis. Figure 2(b) depicts that velocity declines with increasing m. In Figure 2(c), it is seen that velocity increments with enhancing values of Q. Figure 2(d) shows the decline in velocity for increasing U_{HS}. Moreover, velocity

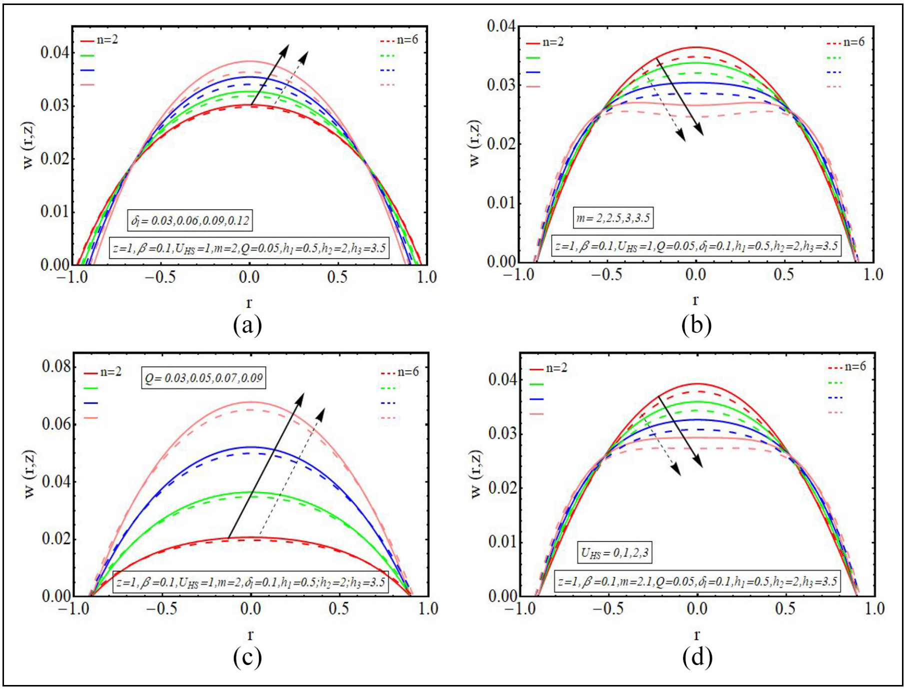

Figure 2. (a) Velocity for δ_l, (b) velocity for m, (c) velocity for Q, and (d) velocity for U_{HS}.

attains its highest value for zero U_{HS} and gradually declines with enhancing value of U_{HS}. Thus, the speed of flow can mainly be governed by electric field that is axially applied. It is seen in these graphs of velocity that the increase in velocity is less for non-uniform shape as compared to uniform shape of multiple stenosis. The shear stresses at walls having multiple stenosis are plotted for various parameters and shown in Figure 3(a)–(d). The value of τ_w increments with increasing δ_l, provided in Figure 3(a). Also, there is enhance in τ_w with increasing electro-kinetic parameter m, given in Figure 3(b). Figure 3(c) convey that τ_w gains magnitude, as the flow rate Q enhances. In Figure 3(d), it is noted that τ_w increments for incrementing value of U_{HS}. The shear stress increases in all cases mainly due to "no slip" at walls. In Figure 4(a)–(f), the temperature graphs are displayed for varying values of involved parameters. Figure 4(a) shows enhance in temperature with incrementing B_r. Figure 4(b) depicts that there is enhance in temperature at the center but declines with walls having multiple stenosis, as the value of δ_l increases. There is decrease in temperature with incrementing m, displayed in Figure 4(c). The temperature gains magnitude for enhancing values of Q, given in Figure 4(d). Figure 4(e) depicts enhance in temperature with enhancing Joule heating S. There is

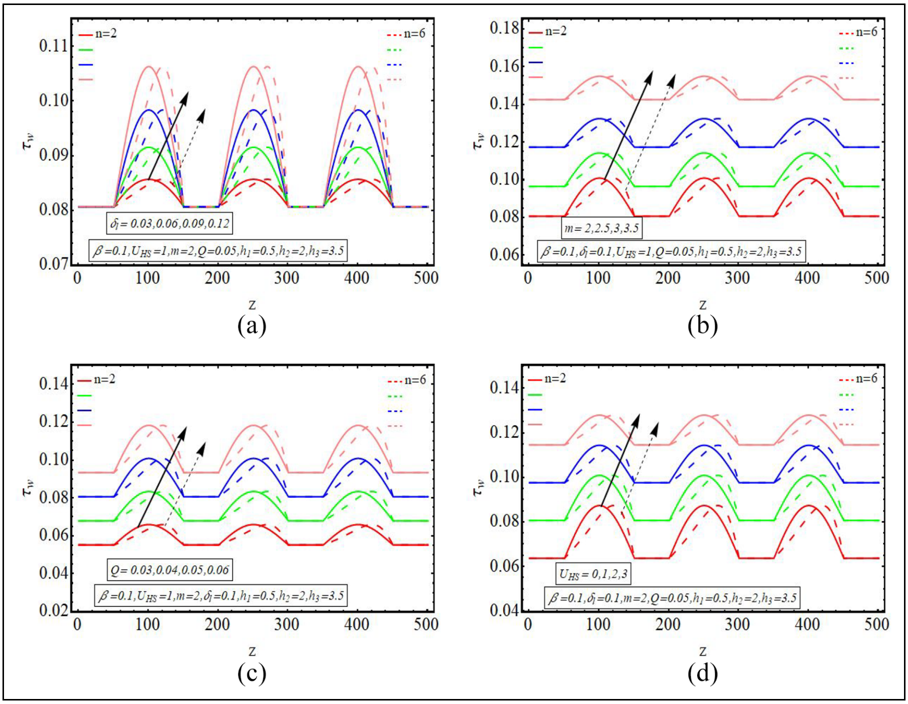

Figure 3. (a) τ_w for δ_l, (b) τ_w for m, (c) τ_w for Q, and (d) τ_w for U_{HS}.

decline in temperature, as the values of U_{HS} increases, as shown in Figure 4(f). All these temperature graphs reveal that the increment in temperature for uniform shape of multiple stenosis is higher when compared with non-uniform shape. Further, both velocity as well as temperature declines with increasing axial electric field. Thus, the flow can be controlled interms of both speed and temperature by application of electro-osmosis. Figure 5(a)–(d) show streamline graphs for increasing values of electro-osmosis parameter m, while both symmetric as well as non-symmetric shapes of multiple stenosis are considered. The trapping declines in size with incrementing m, for symmetric shape of stenosis. But there is enhance in size of trapped streamlines, for non-symmetric case. Further, the walls with multiple stenosis can clearly be seen in these streamlines. Also, the symmetric and non-symmetric shapes are clearly observed. The streamlines for flow rate Q are also plotted and provided in Figure 6(a)–(d). When the multiple stenosis have symmetric shape, then there is enhance in size of trapping with incrementing Q. But when the shape is non-symmetric then the trapping declines in size for increasing Q. Moreover, when the multiple stenosis have symmetric shape then the trapping pattern is also symmetric in shape but it turns to be non-symmetric in shape, when the multiple stenosis have non-symmetric shape.

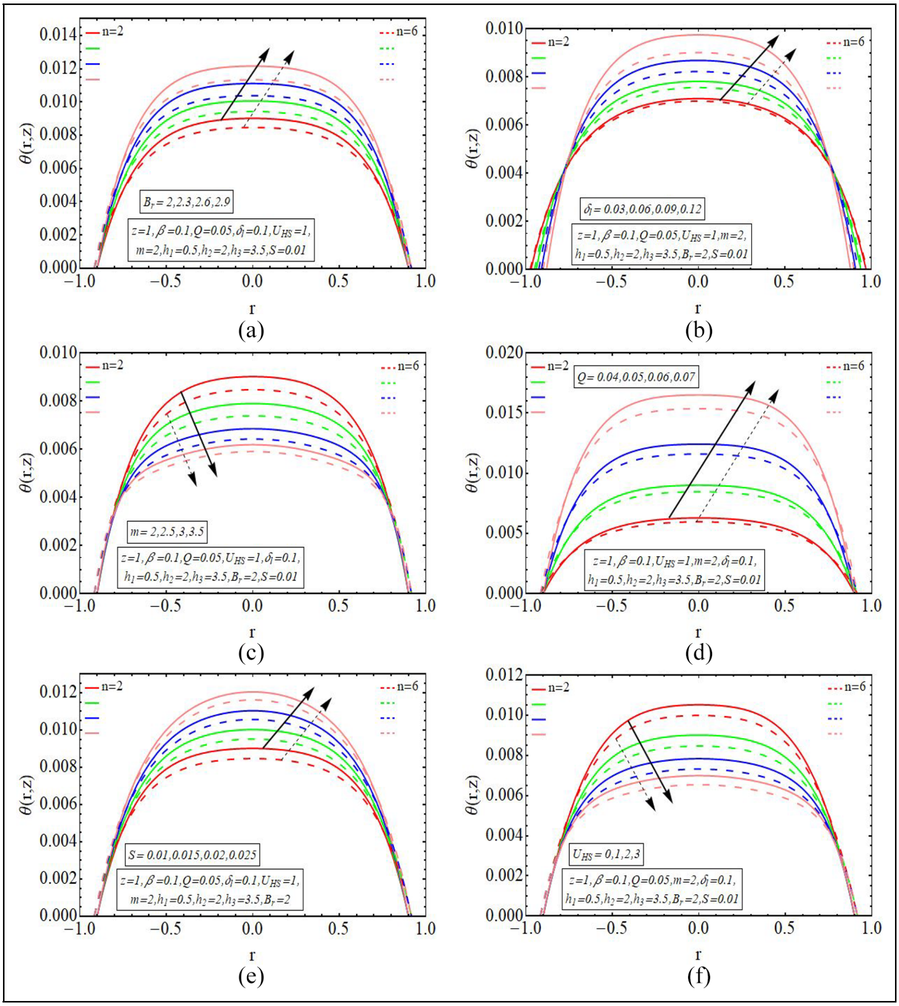

Figure 4. (a) Temperature for B_r, (b) temperature for δ_l, (c) temperature for m, (d) temperature for Q, (e) temperature for S, and (f) temperature for U_{HS}.

Conclusions

The electro-osmotically developed hemodynamics across an artery with multiple stenosis is examined. The non-Newtonian behaviour of blood is incorporated by using Casson fluid model. The important results are

- The speed of flow can mainly be governed by electric field that is axially applied.

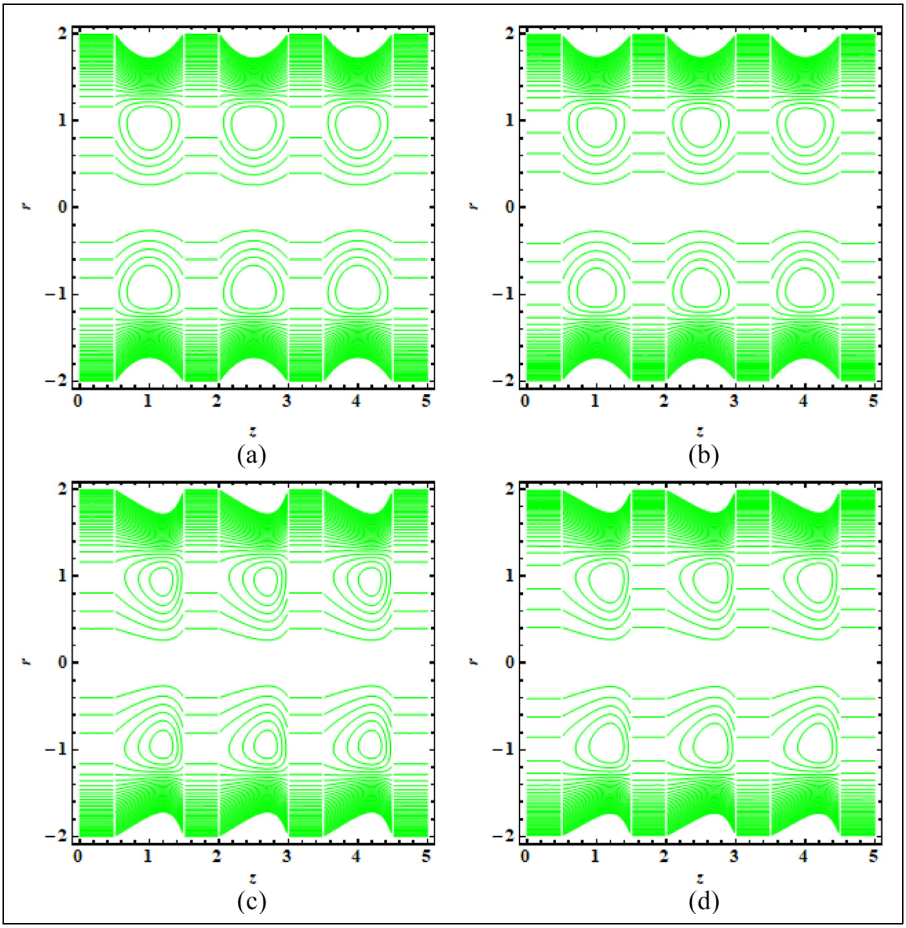

Figure 5. (a) Streamlines for $m = 2, n = 2$, (b) streamlines for $m = 3, n = 2$, (c) streamlines for $m = 2, n = 6$, and (d) streamlines for $m = 3, n = 6$.

- The enhance in velocity is less for non-uniform shape as compared to uniform shape of multiple stenosis.
- The medical advantages of electro-osmosis include treatment of cellular anomalies, sickle cells and delivery of drugs, etc.
- The present analysis is limited due to theoretical approach and there is no experimental work performed during this research.
- The flow can be controlled interms of both speed and temperature by application of electro-osmosis.
- The multiple stenosis have symmetric shape then the trapping is also symmetric in shape but it turns to be non-symmetric in shape, when the multiple stenosis have non-symmetric shape.

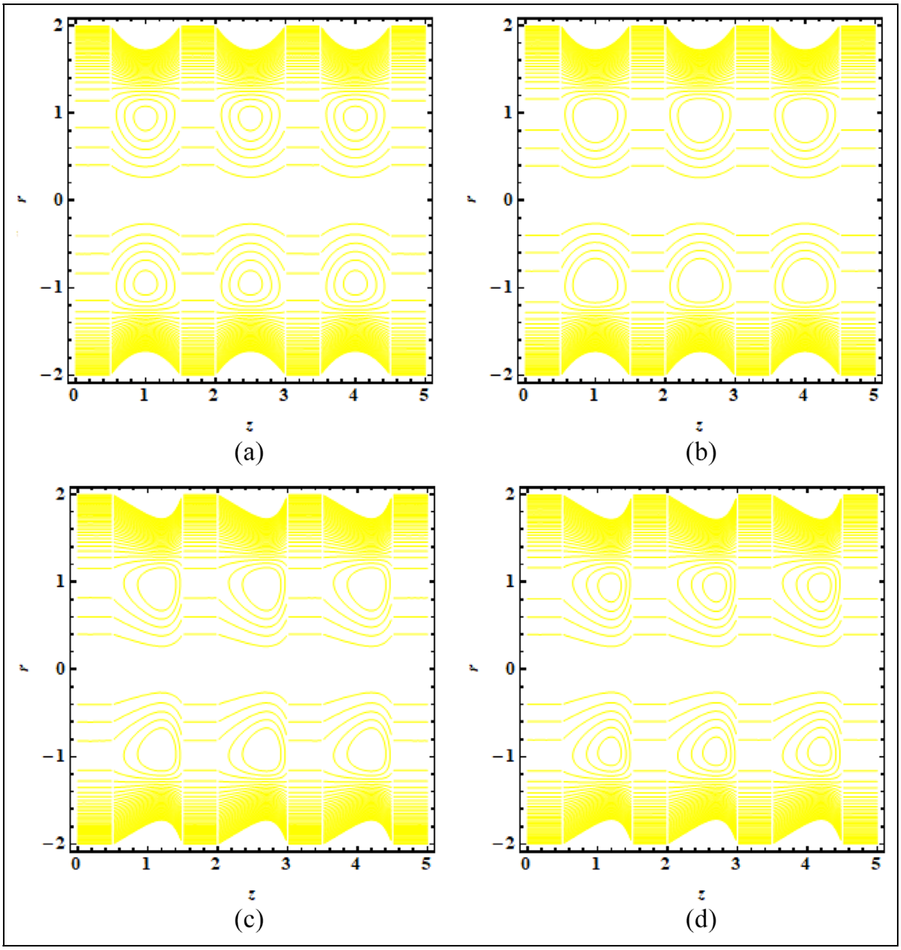

Figure 6. (a) Streamlines for $Q = 1, n = 2$, (b) streamlines for $Q = 2, n = 2$, (c) streamlines for $Q = 1, n = 6$, and (d) streamlines for $Q = 2, n = 6$.

Declaration of conflicting interests

The author(s) declared no potential conflicts of interest with respect to the research, authorship, and/or publication of this article.

Funding

The author(s) disclosed receipt of the following financial support for the research, authorship, and/or publication of this article: The author Salman Saleem extends his appreciation to the Deanship of Scientific research at King Khalid University for funding this work through research grant program under Grant no. RGP.2/38/42.

ORCID iDs

Sohail Nadeem https://orcid.org/0000-0002-7388-3946
Alibek Issakhov https://orcid.org/0000-0002-1937-8615

References

1. Huang X, Gordon MJ and Zare RN. Current-monitoring method for measuring the electroosmotic flow rate in capillary zone electrophoresis. *Anal Chem* 1988; 60(17): 1837–1838.
2. Minerick AR, Ostafin AE and Chang HC. Electrokinetic transport of red blood cells in microcapillaries. *Electrophoresis* 2002; 23(14): 2165–2173.
3. Dolník V, Liu S and Jovanovich S. Capillary electrophoresis on microchip. *Electrophoresis* 2000; 21(1): 41–54.
4. Wu RC and Papadopoulos KD. Electroosmotic flow through porous media: cylindrical and annular models. *Colloid Surf A Physicochem Eng Asp* 2000; 161(3): 469–476.
5. Yang RJ, Fu LM and Lin YC. Electroosmotic flow in microchannels. *J Colloid Interf Sci* 2001; 239(1): 98–105.
6. Zhao C, Zholkovskij E, Masliyah JH, et al. Analysis of electroosmotic flow of power-law fluids in a slit microchannel. *J Colloid Interf Sci* 2008; 326(2): 503–510.
7. Tang GH, Li XF, He YL, et al. Electroosmotic flow of non-Newtonian fluid in microchannels. *J Non-Newtonian Fluid Mech* 2009; 157(1–2): 133–137.
8. Liu Q, Jian Y and Yang L. Alternating current electroosmotic flow of the Jeffreys fluids through a slit microchannel. *Phys Fluids* 2011; 23(10): 102001.
9. Nadeem S, Kiani MN, Saleem A, et al. Microvascular blood flow with heat transfer in a wavy channel having electroosmotic effects. *Electrophoresis* 2020; 41(13–14): 1198–1205.
10. Narla VK and Tripathi D. Electroosmosis modulated transient blood flow in curved microvessels: study of a mathematical model. *Microvasc Res* 2019; 123: 25–34.
11. Tripathi D, Yadav A, Bég OA, et al. Study of microvascular non-Newtonian blood flow modulated by electroosmosis. *Microvasc Res* 2018; 117: 28–36.
12. Akram J, Akbar NS and Maraj EN. A comparative study on the role of nanoparticle dispersion in electroosmosis regulated peristaltic flow of water. *Alex Eng J* 2020; 59(2): 943–956.
13. Saleem S, Akhtar S, Nadeem S, et al. Mathematical study of Electroosmotically driven peristaltic flow of Casson fluid inside a tube having systematically contracting and relaxing sinusoidal heated walls. *Chin J Phys* 2021; 71: 300–311.
14. Ponalagusamy R. *Blood flow through stenosed tube*. PhD Thesis, IIT, Bombay, India, 1986.
15. Ponalagusamy R. Blood flow through an artery with mild stenosis: a two-layered model, different shapes of stenoses and slip velocity at the wall. *J Appl Sci* 2007; 7(7): 1071–1077.
16. Varshney G, Katiyar V and Kumar S. Effect of magnetic field on the blood flow in artery having multiple stenosis: a numerical study. *Int J Eng Sci Technol* 2010; 2(2): 967–982.
17. Sreenadh S, Pallavi AR and Satyanarayana BH. Flow of a Casson fluid through an inclined tube of non-uniform cross section with multiple stenoses. *Adv Appl Sci Res* 2011; 2(5): 340–349.

18. Nadeem S and Ijaz S. Single wall carbon nanotube (SWCNT) examination on blood flow through a multiple stenosed artery with variable nanofluid viscosity. *AIP Adv* 2015; 5(10): 107217.
19. Akbar NS, Nadeem S and Ali M. Jeffrey fluid model for blood flow through a tapered artery with a stenosis. *J Mech Med Biol* 2011; 11(3): 529–545.
20. Akbar NS and Nadeem S. Carreau fluid model for blood flow through a tapered artery with a stenosis. *Ain Shams Eng J* 2014; 5(4): 1307–1316.
21. Akbar NS and Nadeem S. Simulation of heat and chemical reactions on Reiner Rivlin fluid model for blood flow through a tapered artery with a stenosis. *Heat Mass Transf* 2010; 46(5): 531–539.
22. Toghraie D, Esfahani NN, Zarringhalam M, et al. Blood flow analysis inside different arteries using non-Newtonian Sisko model for application in biomedical engineering. *Comput Methods Programs Biomed* 2020; 190: 105338.
23. Yan SR, Zarringhalam M, Toghraie D, et al. Numerical investigation of non-Newtonian blood flow within an artery with cone shape of stenosis in various stenosis angles. *Comput Methods Programs Biomed* 2020; 192: 105434.
24. Yan SR, Sedeh S, Toghraie D, et al. Analysis and management of laminar blood flow inside a cerebral blood vessel using a finite volume software program for biomedical engineering. *Comput Methods Programs Biomed* 2020; 190: 105384.
25. Foong LK, Shirani N, Toghraie D, et al.. Numerical simulation of blood flow inside an artery under applying constant heat flux using Newtonian and non-Newtonian approaches for biomedical engineering. *Comput Methods Programs Biomed* 2020; 190: 105375.
26. Foong LK, Zarringhalam M, Toghraie D, et al. Numerical study for blood rheology inside an artery: the effects of stenosis and radius on the flow behavior. *Comput Methods Programs Biomed* 2020; 193: 105457.
27. Karimipour A, Toghraie D, Abdulkareem LA, et al. Roll of stenosis severity, artery radius and blood fluid behavior on the flow velocity in the arteries: application in biomedical engineering. *Med Hypotheses* 2020; 144: 109864.
28. Tashtoush B and Magableh A. Magnetic field effect on heat transfer and fluid flow characteristics of blood flow in multi-stenosis arteries. *Heat Mass Transf* 2008; 44(3): 297–304.
29. Ponalagusamy R and Selvi RT. Influence of magnetic field and heat transfer on two-phase fluid model for oscillatory blood flow in an arterial stenosis. *Meccanica* 2015; 50(4): 927–943.
30. Akbar NS, Nadeem S and Lee C. Influence of heat transfer and chemical reactions on Williamson fluid model for blood flow through a tapered artery with a stenosis. *Asian J Chem* 2012; 24(6): 2433–2441.
31. Sadeghi A and Saidi MH. Viscous dissipation effects on thermal transport characteristics of combined pressure and electroosmotically driven flow in microchannels. *Int J Heat Mass Transf* 2010; 53(19–20): 3782–3791.
32. Li Z, Shahsavar A, Niazi K, et al. The effects of vertical and horizontal sources on heat transfer and entropy generation in an inclined triangular enclosure filled with non-Newtonian fluid and subjected to magnetic field. *Powder Technol* 2020; 364: 924–942.
33. Ho CJ, Liu YC, Yang TF, et al. Convective heat transfer of nano-encapsulated phase change material suspension in a divergent minichannel heatsink. *Int J Heat Mass Transf* 2021; 165: 120717.

34. Ho CJ, Liu YC, Ghalambaz M, et al. Forced convection heat transfer of Nano-Encapsulated Phase Change Material (NEPCM) suspension in a mini-channel heatsink. *Int J Heat Mass Transf* 2020; 155: 119858.
35. Chien LH, Cheng YT, Lai YL, et al. Experimental and numerical study on convective boiling in a staggered array of micro pin-fin microgap. *Int J Heat Mass Transf* 2020; 149: 119203.
36. Mekheimer KS, Haroun MH and Elkot MA. Effects of magnetic field, porosity, and wall properties for anisotropically elastic multi-stenosis arteries on blood flow characteristics. *Appl Math Mech* 2011; 32(8): 1047.
37. Nadeem S, Haq RU and Lee C. MHD flow of a Casson fluid over an exponentially shrinking sheet. *Sci Iran* 2012; 19(6): 1550–1553.
38. Liechty BC, Webb BW and Maynes RD. Convective heat transfer characteristics of electro-osmotically generated flow in microtubes at high wall potential. *Int J Heat Mass Transf* 2005; 48(12): 2360–2371.

Appendix

Notations

$(\bar{r}, \bar{z})$	cylindrical coordinate system
$(\bar{u}, \bar{w})$	radial and axial velocity components
R	non-stenotic radius of artery
d_l	stenosis position ($l = 1, 2, 3$)
s_l	stenosis length ($l = 1, 2, 3$)
B_r	Brickman number
λ_d	Debye-length
E_z	axial electrical field
n_0	ions concentration
U_{HS}	Helmholtz-Smoluchowski velocity
z^*	charge balance
i_e	current density
n^+, n^-	cation and anion densities
ζ	zeta potential
μ_B	plastic viscosity
$n \geqslant 2$	multiple stenosis shape parameter
$n = 2$	symmetric shape of multiple stenosis
$n = 6$	non-symmetric shape of multiple stenosis
δ_l^*	maximum height of stenosis in dimensional form
σ	electrical resistivity of fluid
ρ_e	density of total ionic charge
T^*	average temperature of electrolyte solution
e	electronic charge
K_B	Boltzmann Constant
S	Joule heating parameter
m	electro-osmotic parameter
E	permittivity

$\bar{\Phi}$	electro-kinetic potential function
β	Casson parameter
p_y	yield stress

Author biographies

Salman Akhtar is a PhD research fellow at Quaid-i-Azam University, Islamabad, Pakistan. His field of research is applied mathematics and computational fluid mechanics. He has published many articles under the supervision of Prof. Sohail Nadeem.

Luthais B McCash is an Honorary Fellow at the University of Leicester. He was previously the Lead Data Scientist and Head of the Mathematical Modelling, Simulation & Computation at a Scottish Energy company. Although he is interested in Applied and Industrial Mathematics in general, Luthais' current research focuses on quantum fluids, and applied PDEs. Currently he collaborates with colleagues in both Leicester and externally.

Sohail Nadeem is a professor and chairman of department of Mathematics at Quaid-i-Azam University, Islamabad, Pakistan. His field of research is applied mathematics and computational fluid mechanics. His contribution to the field is recognized at national and international levels. He has produced a good number of PhD students. Also, he is serving as editor of various well reputed international journals.

Salman Saleem earned his PhD degree in Mathematics and presently working as an Assistant Professor at King Khalid University, Saudi Arabia. His area of research is computational fluid mechanics. He has published a good number of articles and serving as editor of Hindawi journals.

Alibek Issakhov is currently working Head of Department at Alfarabi Kazkh National University, Kazakhstan. He is a scholar, researcher, and teacher per excellence. He has authored many research articles which show his excellence in the field.